buildings

MDPI

Article

Building Vibration Measurement and Prediction during Train Operations

Lingshan He [1] and Ziyu Tao [2,*]

[1] Guangzhou Urban Planning & Design Survey Research Institute Co., Ltd., Guangzhou 510000, China; zacharyhe@foxmail.com
[2] Department of Civil and Environmental Engineering, The Hong Kong Polytechnic University, Hong Kong 999077, China
* Correspondence: zi-yu.tao@polyu.edu.hk

Abstract: Urban societies face the challenge of working and living in environments filled with vibration caused by transportation systems. This paper conducted field measurements to obtain the characteristics of vibration transmission from soil to building foundations and within building floors. Subsequently, a prediction method was developed to anticipate building vibrations by considering the soil and structure interaction. The rigid foundation model was simplified into a foundation–soil system connected via spring damping, and the building model is based on axial wave transmission within the columns and attached floors. Building vibrations were in response to measured input vibration levels at the ground and were validated through field measurements. The influence of different building heights on soil and structure vibration propagation was studied. The results showed that the predicted vibrations match well with the measured vibrations. The proposed prediction model can reasonably predict the building vibration caused by train operations. The closed-form method is an efficient tool for predicting floor vibrations prior to construction.

Keywords: train-induced vibration; soil–structure interaction; prediction model; vibration measurement

Citation: He, L.; Tao, Z. Building Vibration Measurement and Prediction during Train Operations. *Buildings* **2024**, *14*, 142. https://doi.org/10.3390/buildings14010142

Academic Editor: Shaohong Cheng

Received: 21 December 2023
Revised: 29 December 2023
Accepted: 5 January 2024
Published: 6 January 2024

1. Introduction

Transport-oriented development (TOD) has been widely promoted and applied in urban rail transit infrastructure, including lines, stations, and metro depots, improving the development layout of the subway, community, and industry [1,2]. This procedure allows the surrounding properties to fully enjoy the dividends of rail transit and further shortens the distance between rail transit and buildings. However, as the distance between the vibration source and the building is reduced, the impact of the train operation on the building's vibration is further intensified, which has become one of the core problems to be controlled in the development of rail transit.

The rapid and accurate prediction of long-term environmental vibration caused by train operation and effective guidance for comprehensive vibration reduction and isolation design are the basis for promoting the rapid and benign development of rail transit properties [3,4]. To accurately calculate the building vibration effects, it is necessary to find out the propagation mechanism of vibration in the vibration source, soil, and building. The dynamic interaction between soil and structure is the key factor in determining vibration propagation.

Most existing models usually ignore the coupling between the vibration source and the building [5–7]. In structural design, the boundary condition is usually a fixed base, but in practice, the foundation soil is not completely rigid. Considering the subsoil, foundation structure, and superstructure as a unified dynamic system, the actual stiffness of the subsoil is introduced by considering the deformation ability, and the natural frequency of the system will be reduced [8]. Therefore, considering the dynamic coupling between foundation soil and structure has practical significance in the vibration response of building

structures [9–11]. Kuo et al. [12] characterized the dynamic coupling between soil and structure through coupling loss, and defined it as the difference in vibration levels inside and outside the building. Francois et al. [13] studied the influence of dynamic coupling between soil and structure on adjacent buildings and showed that assuming that the building base and the incident wave field movement were consistent could distort calculated vibrations. Coulier et al. [14] showed that when the distance between the vibration source and the building is smaller than the wavelength in the soil, the coupling effect between the soil and the shallow foundation of the building is very significant, and the interaction with the pile foundation is expected to be greater.

The dynamic coupling between soil and structure is investigated through the global analysis method or substructure method [15–17]. The global analysis method takes the structure and foundation soil as a complete dynamic system. However, due to the complexity of the problem, this method can only be realized via numerical simulation. Its disadvantage is that the modeling workload and calculation costs are large, making it challenging for application in large-scale engineering practice. The substructure method models the structure and the foundation independently and calculates the substructure model separately to solve the dynamic response of the superstructure by introducing the boundary conditions of the contact between the soil and the foundation, which offers the advantages of reduced computing memory requirements and higher efficiency [18]. Based on the substructure method, Fiala et al. [19] studied the vibration and radiated noise response of adjacent frame structures caused by train operations. The dynamic coupling between soil and structure was considered by coupling the impedance function of soil in the building base as the boundary condition. Lopes et al. [20] studied the response of soil stiffness to ground frame structure vibrations caused by tunnel train operations under the consideration of the dynamic coupling of soil and structure through numerical simulation. The dynamic coupling of soil and structure was simulated via the boundary element method and the simplified lumped parameter method, respectively. Considering the dynamic interaction between soil and structure is a crucial factor in accurately predicting structural vibration response. Ignoring this effect may result in overly conservative prediction outcomes.

Furthermore, the key to the method of calculating the environmental vibration of rail transit is to improve calculation accuracy, which requires a balance between time and accuracy [21–24]. The use of physical transfer functions to evaluate vibration effects is reliable and effective, and Connolly et al. [25] synthesized thousands of vibration data records from seven European countries to confirm this view. The physical properties of soil mass are the most important factors affecting vibration calculation. However, it is difficult to obtain a large number of the field test data needed to establish physical transfer functions in engineering practice, so the transfer function method has not been widely used in environmental vibration prediction. In the past decade, numerical modeling has been widely used in the field of environmental vibration [26]. Traditional numerical models need to integrate three components: vibration source, vibration transmission path, and building structure [27,28], which can usually be divided into two parts: the vehicle–track–soil coupling model and soil–structure coupling model. To find a balance between prediction accuracy and prediction time cost, scholars from various countries have conducted a lot of model simplification and algorithm optimization work, such as the finite-boundary element model [29], 2.5D finite element model [30,31], and finite difference model [32]. Due to the uncertainty of many parameters in numerical models, it is necessary to conduct repeated checks of the model through field test data [33] to calibrate the model parameters.

To solve this problem, a hybrid model vibration prediction method has gradually been developed that combines field testing and vibration theory techniques to avoid errors caused by model simplification. This approach also mitigates the issue of numerical models requiring an excessive number of calculation parameters, and providing a new idea for the environmental vibration prediction of rail transit [34]. Guo et al. [35] established a theoretical model of the building structure for vibration prediction based on the dynamic

stiffness matrix method, allowing the calculation of the frequency domain response. The validity of the model was verified by using the measured data of the parking lot of Nanjing University Town. Sanayei et al. [36,37] described vertical vibration wave conduction by assembling single, independent structural column components and attached floor components, and established a one-dimensional impedance theoretical prediction model with measured building foundation vibration as input. The impedance model was verified via a four-story building scale model composed of aluminum columns and MDF in laboratory experiments and field tests at the Boston Hynes Convention Center. Zou et al. [38] extended the one-dimensional impedance model to a two-dimensional impedance model, taking into account the propagation of axial waves and bending waves in frame columns and shear walls. Later, to consider the influence of the transfer structure on the vibration propagation rule, Zou et al. [39] extended the two-dimensional impedance model to a three-dimensional impedance model under the condition of multiple-load input [40]. The model takes into account the different forms of vibration wave source in the transfer structure more reasonably, which is especially suitable for large high-rise buildings.

The current practice shows that the vibration response of buildings is affected by the type of building foundation and soil layer parameters, and the coupling effect of soil and structure affects the accuracy of the vibration prediction method. In this paper, the characteristics of vibration propagation loss between soil and structure are illustrated through field tests, the influence of train operation on building vibration is predicted by establishing a prediction model, and the influence of different building heights on the vibration propagation of soil and structure is studied. The objective is to develop a methodology involving ground vibration measurements for obtaining the ground vibration response, thereby enabling an accurate prediction of building vibration response during mitigation measure design prior to construction. This approach utilizes ground vibration as a model input, mitigating uncertainties associated with vibration propagation in tunnel and soil layers.

2. Field Measurement

2.1. Measurement Setup

The building that is close to the tunnel of Nanjing Metro Line 3 was selected to carry out the measurements. The horizontal distance between the building and the tunnel is about 40 m, and the buried depth is 17 m. The spatial relationship between the building and the tunnel is shown in Figure 1, and the photo of the building is shown in Figure 2.

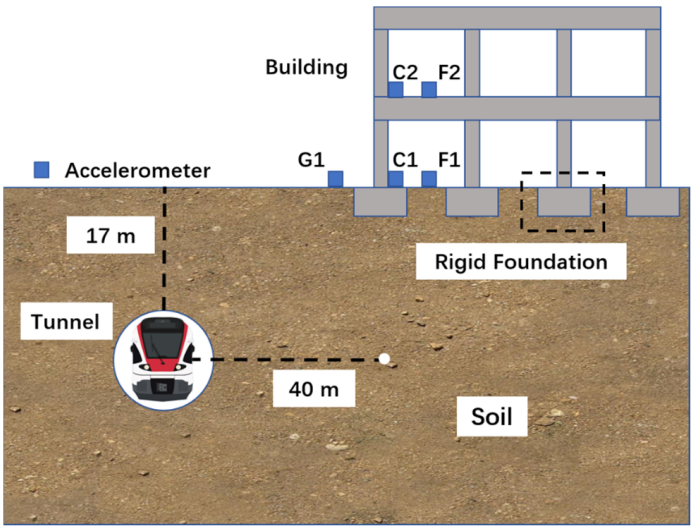

Figure 1. Spatial relationship between the building and the tunnel.

Figure 2. Measured 2-story building.

According to the geological drilling survey data, the soil is divided into four layers: plain fill, clay, muck, and silty clay. Table 1 lists the physical parameters of the soil layer.

Table 1. Physical parameters of the soil layer.

Name	Thickness (m)	Density (kg/m^3)	Poisson's Ratio	Modulus of Elasticity (MPa)
Plain fill	2.1	16	0.45	120
Clay	1.3	18.4	0.46	130
Muck	8.4	17.5	0.48	300
Silty clay	10.6	19.3	0.45	380

The building is a reinforced concrete-frame structure with 2 floors and a height of 8 m, which relies on structural columns for load-bearing with a size of 0.4×0.4 m^2. The building foundation is a rigid foundation with a base size of 1.2×1.2 m^2. Table 2 lists the dimensions and dynamics parameters of the building structure, where h, t, w, E, and ρ are the height, thickness, width, elastic modulus, density of the structural components, respectively. The damping ratio and Poisson's ratio of the reinforced concrete structural components are 0.02 and 0.2, respectively.

Table 2. Physical parameters of the building structure.

Structural Component	h (m)	t (m)	w (m)	E (Gpa)	ρ (kg/m^3)
Column	4	0.4	0.4	32.5	2500
Floor slab	-	0.1	-	30	2500
Rigid foundation	-	1.2	1.2	32.5	2500

A total of 4 measuring points were arranged inside the building and measuring point was arranged outside the building to collect the vibration acceleration caused by train operations, as shown in Figure 1. In total, 20 train pass-by events were recorded, with the trains traveling at approximately 50 km/h. The sampling frequency was set to 512 Hz. The JM3873 wireless acquisition system was selected as the accelerometer which is made by the Jing Ming Technology, Yangzhou, China, as shown in Figure 3. The duration of measurement was a working day with a relatively low pedestrian flow. During the measurements, the weather conditions were characterized by clear skies and low wind speeds.

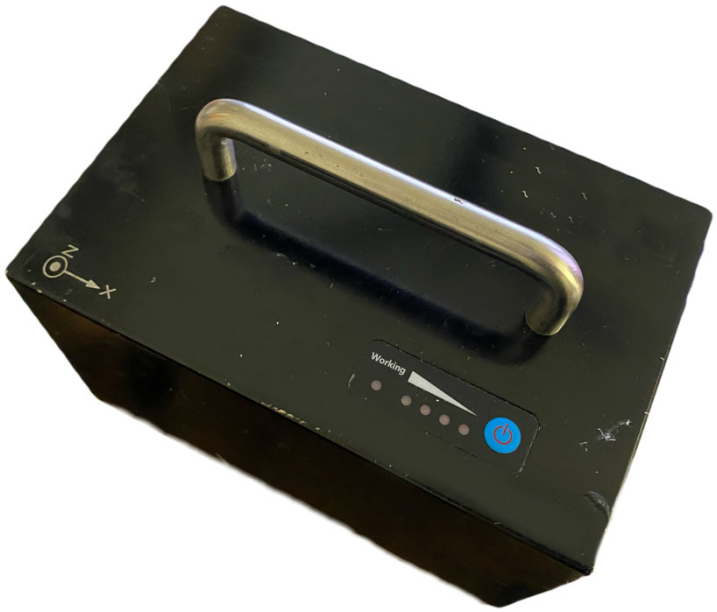

Figure 3. Accelerometer.

2.2. Measurement Results

The time history of acceleration of each measuring point caused by train operations is separated from the records of continuous synchronous testing, and the typically measured time history of a train pass-by event is shown in Figure 4.

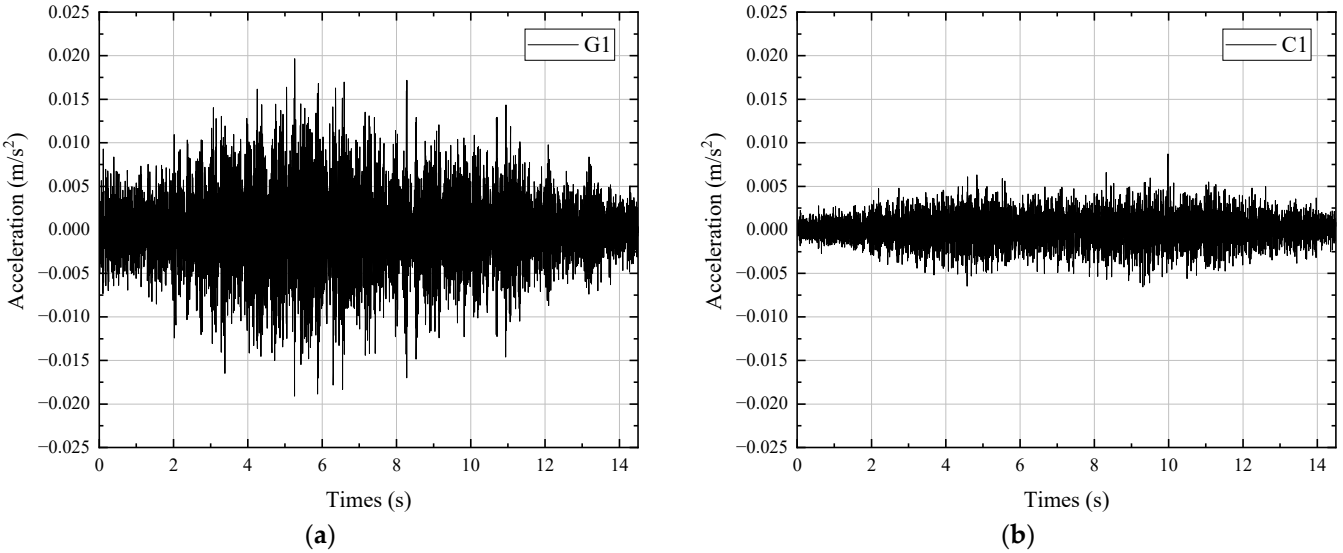

Figure 4. Measured typical time history of acceleration. (**a**) Ground G1; (**b**) 1st-floor C1.

The duration of ground and building vibrations caused by train operation is about 14.5 s. The ground vibration with a peak acceleration of about 0.02 m/s^2 is greater than the column vibration with a peak acceleration of about 0.008 m/s^2.

The measured acceleration is calculated and converted into a 1/3 octave band to obtain the vertical vibration acceleration level. The acceleration levels are presented in the form of an envelope diagram to show the influence range caused by different train pass-by events, as shown in Figure 5.

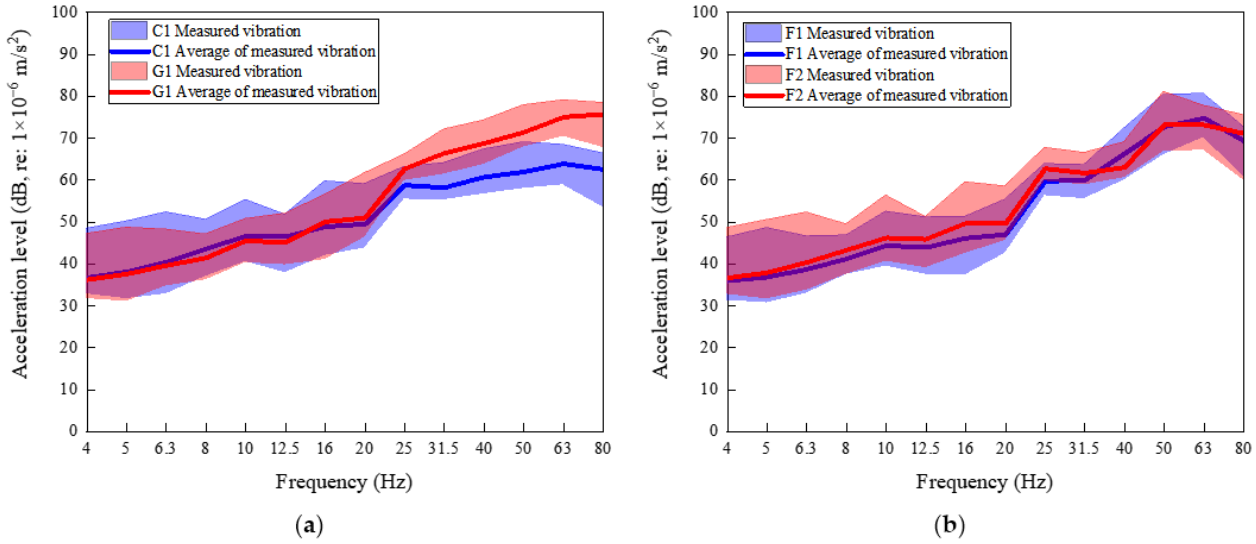

Figure 5. Measured acceleration levels of a 1/3 octave band frequency. (**a**) Comparison of ground vibration and column vibration on 1st floor; (**b**) comparison of floor vibration on 1st floor and 2nd floor.

Comparing the location of G1 and C1 in Figure 5a, the vibration loss of vibration propagating from the soil to the structure is more obvious, and it tends to decrease significantly at a high frequency, while the attenuation of middle and low frequencies is not obvious. The dividing line is at 25 Hz, and the vibration acceleration level above 25 Hz decreases significantly.

Comparing the location of F1 and F2, with the increase in building height, the difference in vibration acceleration in the frequency domain is not obvious. In the propagation process, the characteristic frequencies are consistent, which is because the floor height is small and the building system tends to be excited as a whole, and the difference in vibration acceleration between the first and second floors is small. In addition, due to the small mass and volume of the building foundation compared with those of the soil, it can be regarded as the interaction between the building structure as a whole and the soil.

3. Vibration Prediction and Validation

To predict the building vibrations, this paper presents a hybrid prediction method based on the measured ground vibration and the prediction model of a building structure that considers the soil–structure interaction. The purpose is that the vibration response of the new building can be calculated via the prediction model of a building structure after the measured vibrations of ground soil surface are obtained. The advantage of this method is that tunnels and different soil layers do not need to be considered in the model, because the foundation of the building is buried in the topsoil, and the vibration of the topsoil surface is obtained via measurement. Hence, a prerequisite of this method is to obtain the measured data of ground vibration.

This model can greatly improve the efficiency of solving the coupling loss between the rigid foundation, soil, and structure. Firstly, the coupling model at the interface between a rigid foundation and soil is simplified as a spring-damping coupling component. The soil layer, where the rigid foundation is located, is considered homogeneous soil, and its parameters aligned with those of the surface soil layer. Subsequently, by adding the building structure to the top of the foundation and considering the influence of the building structure on the coupling loss, the coupling loss of the soil–foundation system under the influence of the building structure is obtained. Finally, the vibration response of the foundation is solved according to the in situ measured ground vibration and soil–foundation coupling loss, and the building response is solved based on the building prediction model. The model diagram is shown in Figure 6.

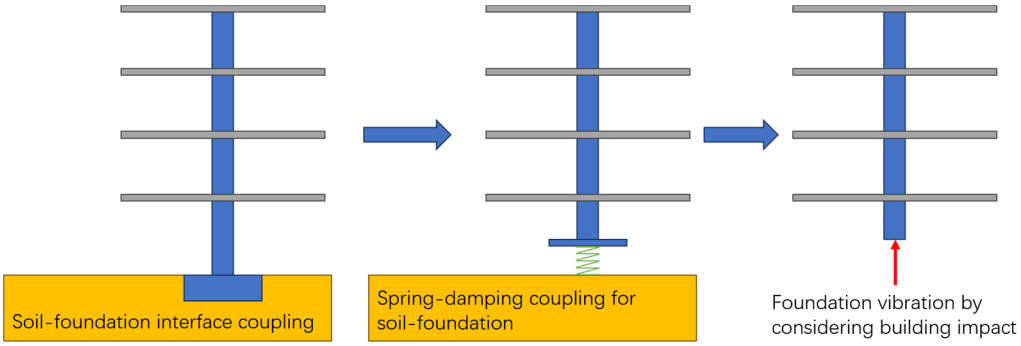

Figure 6. Schematic diagram of vibration prediction model for rigid foundation and building.

3.1. Prediction Model

3.1.1. Soil–Structure Interaction Model

For a rigid foundation, where the contact area between the foundation and soil is small, the dynamic interaction between them is weaker than the inertial interaction of the superstructure, and the influence of soil layer interface on the soil–structure interaction is lower. Therefore, the rigid foundation model can be simplified into a foundation–soil system connected via spring damping. The empirical formula based on boundary element research by Auersch [41] can describe the dynamic behavior of the shallow foundation and soil, and its expression is as follows:

$$k \approx 3.4 G_s \sqrt{A_s} \tag{1}$$

$$c \approx 1.6 \rho_s v_s A_s \tag{2}$$

where A_s is the area of the foundation; G_s, ρ_s, and v_s are the shear modulus, density, and shear wave velocity of soil, respectively. k and c are the stiffness and damping of the foundation, respectively.

Due to the large proportion of building quality being in the building–rigid foundation system, foundation modeling cannot be conducted at the base–structure node without ignoring the influence of the building. For the load-bearing column, the dynamical behavior can be described by the following governing equation:

$$-E_c A_c u''(x_s) = k(u - u_0) + c(u - u_0) \tag{3}$$

where primes and dots denote spatial and time derivatives. u, E_c, and A_c are the vertical displacement, modulus of elasticity, and area of the column, respectively. u_0 is a free-field displacement.

Its solution can be expressed by the following equation:

$$\frac{u_c}{u_0} = \frac{\cos a\xi}{\cos a} \frac{1}{1 + iq \tan a} \tag{4}$$

where u_c is column displacement. i is equal to $\sqrt{-1}$. $\xi = x/H$ is the position relative to building height, H. x is the distance from the roof. $a = 2\pi f H / v_L$ is the normalized frequency parameter. f is the frequency. $v_L = E_c/\rho_c$ is the wave speed of the column. ρ_c is the density of the column. The expression for parameter q is defined as follows:

$$q = \frac{\sqrt{E_c \rho_c} A_c}{1.6 \sqrt{G_s \rho_s} A_s} \tag{5}$$

3.1.2. Building Model

The building model mainly considers the propagation of axial vibration waves in the building, specifically vertical vibrations. Usually, the vibration caused by train operations propagates upward through vertical load-bearing structures, such as structural columns. Since medium- and high-frequency vibration waves can effectively attenuate in the floor, their influence is limited to a short distance from the junction of the vertical load-bearing structure and the floor. Consequently, vibrations have a minimal impact on the mutual propagation of each vertical load-bearing structure. Thus, the propagation of vibration in a building can be considered upward propagation along a single vertical bearing structure with the attached floor, and the vibration of the floor is the sum of the vibration energy carried by each vertical bearing structure. The vibration propagation model can only consider a single vertical bearing structure and each floor. For each component of the building structure, the rod and the plate element can be used to simulate the structural column and the floor slab.

The load-bearing column is simulated as a finite-length rod element with two nodes at a specific frequency, and both ends are connected to adjacent floors. Considering the axial wave propagation in the load-bearing column, the impedance matrix representing the relationship between force and velocity is shown as follows:

$$z_c = \frac{E_c(1+i\eta_c)A_c\beta_c}{iw\sin(\beta_c l_c)}\begin{bmatrix}\cos(\beta_c l_c) & -1\\ -1 & \cos(\beta_c l_c)\end{bmatrix} \tag{6}$$

where $\beta_c = \omega\sqrt{\frac{\rho_c}{E_c(1+i\eta_c)}}$ is the axial wavenumber, ω is the circular frequency, and l_c is the length of the column. E_c and η_c are the elastic modulus and loss factor of the column.

The floor slab and the vertical load-bearing structure are assumed to be rigidly connected and are simulated as infinite plate elements with the same terms under a specific frequency of point load. The impedance expression of the floor is as follows:

$$z_f = 8\sqrt{\frac{\rho_f E_f\left(1+j\eta_f\right)h_f^4}{12\left(1-v_f^2\right)}} \tag{7}$$

where ρ_f, h_f, v_f, E_f, and η_f are the material density, thickness, Poisson's ratio, elastic modulus, and loss factor of the floor, respectively.

3.1.3. System Assembly

The system model is composed by summing the forces and reactions of each component on the node in the vertical direction. Conceptually, this is achieved by considering the force acting on a rigid massless block with an unknown vertical vibration at each node, where the force of each component is achieved by acting on a different surface of the mass block. If there is a vertical external force, it can be applied at each node of the floor slab. The train excitation input is characterized by the force at the bottom column of building on the ground. Hence, to obtain this exciting force, it is necessary to obtain the ground vibration measured on site, and use Equation (4) to obtain the building column vibration at the bottom of the building. Using this building column vibration as the input of the building model, the vibration of each floor of the building can be obtained by solving the following formula:

$$F = ZV \tag{8}$$

where F and V are the external forces and velocity vectors of each floor, respectively; Z is the impedance matrix obtained by cascading Equations (6) and (7) through nodal coupling.

3.2. Model Validation

3.2.1. Transmission Ratio from Soil to Structure

To better compare the effects of soil–structure coupling loss, all time domain signals from ground measuring point G1 and indoor measuring point C4 are analyzed via fast Fourier transform, and the transmission ratio of vibration from soil to building is calculated. On this basis, the proposed model is used to calculate the transmission ratio of vibration from soil to building, and the comparison between the calculated coupling loss and the measured coupling loss is shown in Figure 7a. The coupling loss curve exhibits a peak value around 10–20 Hz, likely attributed to the formant arising from the overall vibration of the building structure and soil. The coupling loss curve moves from a low frequency to a high frequency, and vibration acceleration attenuation moves from a small to large trend. The predicted coupling loss curves closely align with the measured results.

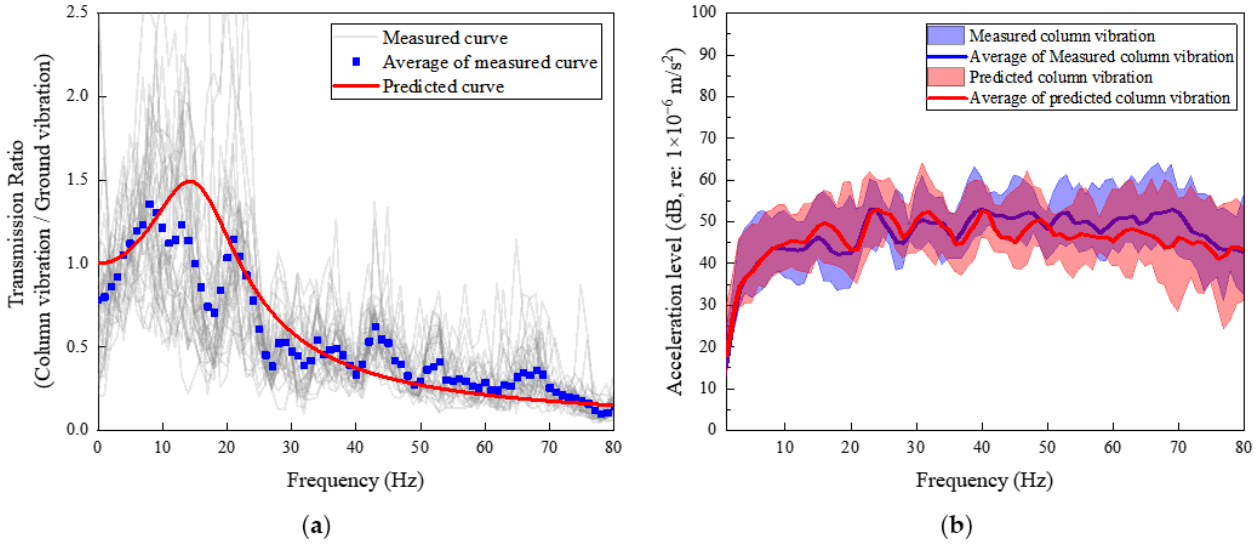

Figure 7. Comparison of measured vibration and predicted vibration from soil to column. (**a**) Transmission ratio; (**b**) column vibration on 1st floor.

By combining the predicted coupling loss curve with the measured ground vibration, the predicted foundation vibration can be obtained, as shown in Figure 7b. The predicted column vibration on the 1st floor is close to the measured vibration. It can be considered that the soil and structure coupling loss can be effectively predicted based on the measured ground vibration and the proposed prediction model.

3.2.2. Building Vibration

For the indoor vibration prediction of the building, measuring points C2 and F2 are selected to represent the column vibration and center of floor vibration, respectively. The envelope diagram and average value of measured and predicted vibrations are compared, as shown in Figure 8.

The predicted vibrations match well with the measured vibrations, and the envelope graph remains consistent across all train pass-by events. The largest discrepancy between the measured average vibration and the predicted average vibration for the column is observed at 80 Hz, exhibiting a difference of 9.2%. Similarly, in terms of floor vibration, the most significant deviation between the measured and predicted average vibrations occurs at 25 Hz, with a disparity of 4.8%. It can be considered that the proposed prediction model can reasonably predict the building vibration caused by train operations.

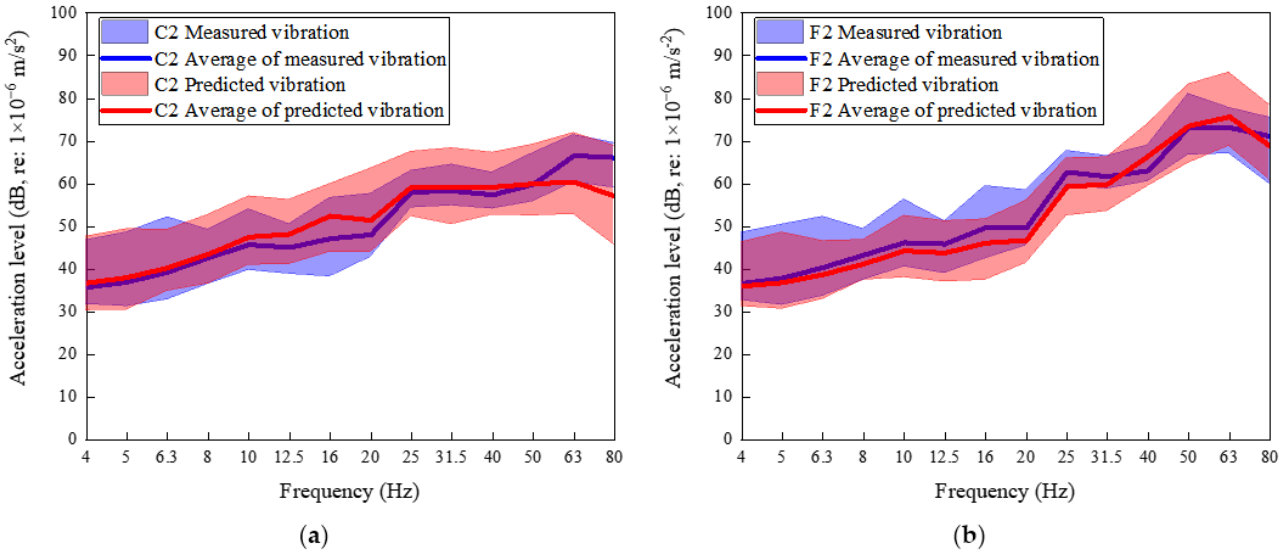

Figure 8. Comparison of measured vibration and predicted vibration within the building (**a**) at the column; (**b**) at the floor center.

4. Discussion

Based on the proposed model, the influence of different building heights on soil–structure interaction is studied by changing the number of building floors. When considering different numbers of floors, since rigid foundations are usually used for shorter buildings, the effects of building height on soil–structure coupling loss are calculated by selecting floors 2, 5, and 8, as shown in Figure 9.

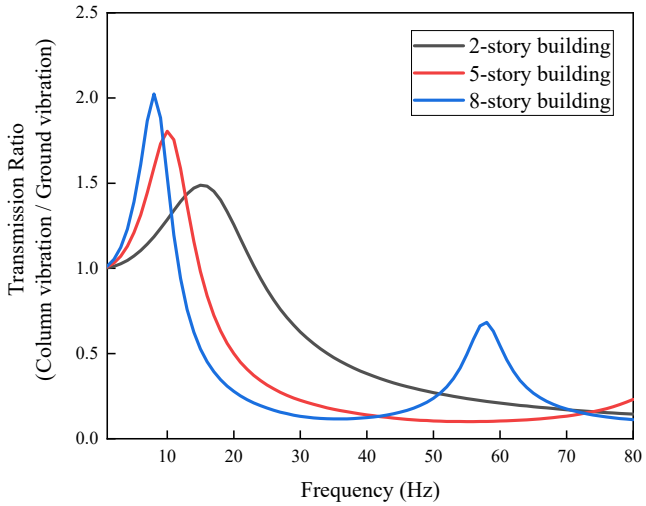

Figure 9. Transmission ratio of soil and structure.

With the increase in the number of floors, the interaction between soil and structure shows an obvious inertia effect. The peak value of the coupling loss curve appears from 20 Hz for a two-story building to 10 Hz for an eight-story building due to the building mass increases. This resonance is attributed to the eigenfrequency of the rigidly founded building, this being approximately 30 Hz, resulting in a 60 Hz elastic building resonance where the foundation and roof vibrate and amplify in an anti-phase [41]. This frequency is controlled by the building height and wave speed of the building column.

Figure 10 compares the difference between the vibration of each floor inside the building and the ground vibration. The vibration of the two-story building shows a gradually increasing trend from the ground floor to the upper floor, but the increase is

very small. In the range of 4–20 Hz, the indoor vibrations are greater than the ground vibration, and the vibration amplification peak is at 16 Hz with a value of about 3 dB. In the range greater than 20 Hz, the ground vibration is greater than indoor vibrations, and the attenuation peak is reached at 80 Hz with about 17 dB.

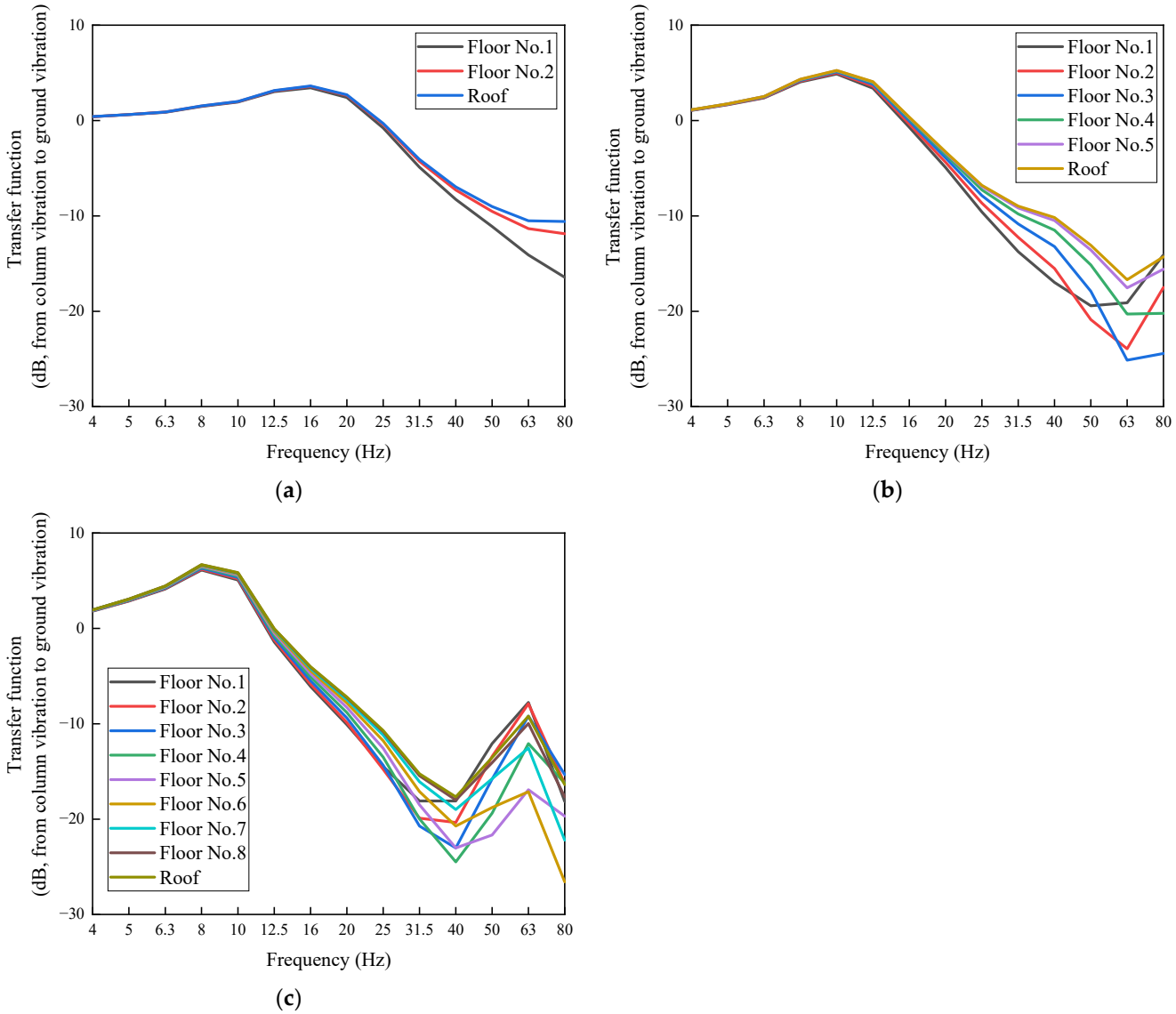

Figure 10. Difference between each floor vibration inside the building and ground vibration. (**a**) Two-story building; (**b**) five-story building; (**c**) eight-story building.

For the five-story building, the propagation law in the building changes, and the overall performance is that the vibration acceleration level of the first floor to the fifth floor decreases first and then increases in the frequency band of 50–80 Hz, and in the range of 4–50 Hz, the acceleration level of the top floor is greater than that of the first floor. In the range of 4–16 Hz, the indoor vibration is greater than the ground vibration with a peak value of 4 dB at 10 Hz. In a range greater than 16 Hz, the ground vibration is greater than the indoor vibration.

For the eight-story building, the low-frequency peak is further increased, and the middle- and high-frequency attenuation capacity is further enhanced. For the propagation in the building, with the increase in the number of floors, the propagation law shows that the vibration acceleration level decreases first and then increases from the 1st floor to the 8th

floor. In the range of 4–12.5 Hz, the indoor vibrations are greater than the ground vibration. In range greater than 12.5 Hz, the ground vibration is greater than the indoor vibrations.

In frame structure buildings, the axial impedance of the load-bearing column far exceeds the bending wave impedance of the floor. Impedance differences appear at the junction of columns and floors on each floor of the building, resulting in a discontinuity of axial impedance. Due to this impedance discontinuity between the high-impedance column and the low-impedance floor, only a small amount of axial upward transmission energy is transferred to the floor. The axial movement of the column in the vertical direction generates floor-bending waves, which propagate outward from the junction of the column and the floor to the outer diameter and are finally dissipated by floor damping. Therefore, in the above analysis of three different building heights, when the number of floors is small, the axial impedance of the column is much larger than that of the floor in the building system. In the propagation process, the vibration propagates along the axis, and the damping of the column itself is not enough to attenuate the vibration, resulting in the vibration energy propagating to the top layer and then being superimposed with the incident wave, resulting in the amplification of the vibration along each layer. As the number of floors increases to a certain height, the damping of the entire building system and the dissipation of each floor will partially attenuate the vibration propagating in the middle floor, so that the vibration decreases first and then increases with building height.

The proposed method also has a limitation; namely, its applicability is restricted to the vibration prediction in newly constructed buildings along operational subway lines, as it necessitates obtaining ground vibrations through field measurements. Furthermore, this method is exclusively suitable for buildings with rigid or shallow foundations due to the previous research on deep foundations revealing distinct soil–structural coupling losses in deep foundation systems, such as pile foundations [42,43].

5. Conclusions

Aiming at the problem of building vibration caused by train operations, a building vibration prediction method considering the coupling loss of soil and structure is established in this paper. Through the field test of the ground and a two-story building that is close to the vibration source, the vibration propagation law in the ground through the building foundation and within the building is obtained, and the validity of the model is verified via measurement. The propagation rules of vibration in buildings with different floors are studied, and the following conclusions are obtained:

(1) The predicted vibration is in good agreement with the measured vibration, and the established prediction model can reasonably predict the vibration of a building with a rigid foundation caused by train operation once the ground vibration can be obtained via measurement.
(2) The coupling loss is obvious as the vibration propagates from the soil to the rigid foundation, and the vibration tends to decrease significantly with an increase in frequency.
(3) For s rigid building foundation, the coupling effect of soil and structure causes a low-frequency building–soil resonance and a high-frequency amplitude attenuation. This effect becomes more pronounced with higher building heights, leading to a more significant change in high-frequency amplitude.

Author Contributions: Conceptualization, L.H. and Z.T.; methodology, Z.T.; validation, Z.T.; formal analysis, L.H.; investigation, L.H.; resources, L.H.; data curation, L.H.; writing—original draft preparation, L.H.; writing—review and editing, Z.T.; visualization, Z.T.; supervision, Z.T.; project administration, Z.T.; funding acquisition, Z.T. All authors have read and agreed to the published version of the manuscript.

Funding: This research was funded by National Natural Science Foundation of China, grant number 51908139.

Data Availability Statement: The data presented in this study are available on request from the corresponding author.

Acknowledgments: The graduate students of Zixiong Shen, Jiahao Hu, Yitao Qiu, and Xuming Li are appreciated for helping us to complete the field measurements.

Conflicts of Interest: Author Lingshan He was employed by the Guangzhou Urban Planning & Design Survey Research Institute Co., Ltd. The remaining authors declare that the research was conducted in the absence of any commercial or financial relationships that could be construed as a potential conflict of interest.

References

1. Zou, C.; Wang, Y.; Moore, J.A.; Sanayei, M. Train-induced field vibration measurements of ground and over-track buildings. *Sci. Total Environ.* **2017**, *575*, 1339–1351. [CrossRef]
2. Zou, C.; Wang, Y.; Wang, P.; Guo, J. Measurement of ground and nearby building vibration and noise induced by trains in a metro depot. *Sci. Total Environ.* **2015**, *536*, 761–773. [CrossRef]
3. He, C.; Zhou, S.; Guo, P. Mitigation of Railway-Induced Vibrations by Using Periodic Wave Impeding Barriers. *Appl. Math. Model.* **2022**, *105*, 496–513. [CrossRef]
4. Liu, Q.; Li, X.; Zhang, X.; Zhou, Y.; Chen, Y.F. Applying Constrained Layer Damping to Reduce Vibration and Noise from a Steel-Concrete Composite Bridge: An Experimental and Numerical Investigation. *J. Sandw. Struct. Mater.* **2020**, *22*, 1743–1769. [CrossRef]
5. Li, X.; Chen, Y.; Zou, C.; Chen, Y. Train-Induced Vibration Mitigation Based on Foundation Improvement. *J. Build. Eng.* **2023**, *76*, 107106. [CrossRef]
6. Liu, Q.; Thompson, D.J.; Xu, P.; Feng, Q.; Li, X. Investigation of Train-Induced Vibration and Noise from a Steel-Concrete Composite Railway Bridge Using a Hybrid Finite Element-Statistical Energy Analysis Method. *J. Sound Vib.* **2020**, *471*, 115197. [CrossRef]
7. Liu, W.; Liang, R.; Zhang, H.; Wu, Z.; Jiang, B. Deep Learning Based Identification and Uncertainty Analysis of Metro Train Induced Ground-Borne Vibration. *Mech. Syst. Signal Process.* **2023**, *189*, 110062. [CrossRef]
8. He, C.; Zhou, S.; Di, H.; Guo, P.; Xiao, J. Analytical Method for Calculation of Ground Vibration from a Tunnel Embedded in a Multi-Layered Half-Space. *Comput. Geotech.* **2018**, *99*, 149–164. [CrossRef]
9. Colaço, A.; Barbosa, D.; Alves Costa, P. Hybrid Soil-Structure Interaction Approach for the Assessment of Vibrations in Buildings Due to Railway Traffic. *Transp. Geotech.* **2022**, *32*, 100691. [CrossRef]
10. Zhou, S.; He, C.; Guo, P.; Yu, F. Dynamic Response of a Segmented Tunnel in Saturated Soil Using a 2.5-D FE-BE Methodology. *Soil Dyn. Earthq. Eng.* **2019**, *120*, 386–397. [CrossRef]
11. Colaço, A.; Alves Costa, P.; Amado-Mendes, P.; Calçada, R. Vibrations Induced by Railway Traffic in Buildings: Experimental Validation of a Sub-Structuring Methodology Based on 2.5D FEM-MFS and 3D FEM. *Eng. Struct.* **2021**, *240*, 112381. [CrossRef]
12. Kuo, K.A.; Papadopoulos, M.; Lombaert, G.; Degrande, G. The Coupling Loss of a Building Subject to Railway Induced Vibrations: Numerical Modelling and Experimental Measurements. *J. Sound Vib.* **2019**, *442*, 459–481. [CrossRef]
13. François, S.; Pyl, L.; Masoumi, H.R.; Degrande, G. The Influence of Dynamic Soil–Structure Interaction on Traffic Induced Vibrations in Buildings. *Soil Dyn. Earthq. Eng.* **2007**, *27*, 655–674. [CrossRef]
14. Coulier, P.; Lombaert, G.; Degrande, G. The Influence of Source–Receiver Interaction on the Numerical Prediction of Railway Induced Vibrations. *J. Sound Vib.* **2014**, *333*, 2520–2538. [CrossRef]
15. Auersch, L. Response to Harmonic Wave Excitation of Finite or Infinite Elastic Plates on a Homogeneous or Layered Half-Space. *Comput. Geotech.* **2013**, *51*, 50–59. [CrossRef]
16. Auersch, L. Dynamic Behavior of Slab Tracks on Homogeneous and Layered Soils and the Reduction of Ground Vibration by Floating Slab Tracks. *J. Eng. Mech.* **2012**, *138*, 923–933. [CrossRef]
17. Auersch, L. Wave Propagation in the Elastic Half-Space Due to an Interior Load and Its Application to Ground Vibration Problems and Buildings on Pile Foundations. *Soil Dyn. Earthq. Eng.* **2010**, *30*, 925–936. [CrossRef]
18. Clot, A.; Arcos, R.; Romeu, J. Efficient three-dimensional building-soil model for the prediction of ground-borne vibrations in buildings. *J. Struct Eng.* **2017**, *143*, 04017098. [CrossRef]
19. Fiala, P.; Degrande, G.; Augusztinovicz, F. Numerical Modelling of Ground-Borne Noise and Vibration in Buildings Due to Surface Rail Traffic. *J. Sound Vib.* **2007**, *301*, 718–738. [CrossRef]
20. Lopes, P.; Alves Costa, P.; Calçada, R.; Silva Cardoso, A. Influence of Soil Stiffness on Building Vibrations Due to Railway Traffic in Tunnels: Numerical Study. *Comput. Geotech.* **2014**, *61*, 277–291. [CrossRef]
21. Papadopoulos, M.; François, S.; Degrande, G.; Lombaert, G. The Influence of Uncertain Local Subsoil Conditions on the Response of Buildings to Ground Vibration. *J. Sound Vib.* **2018**, *418*, 200–220. [CrossRef]
22. Edirisinghe, T.L.; Talbot, J.P. The Significance of Source-Receiver Interaction in the Response of Piled Foundations to Ground-Borne Vibration from Underground Railways. *J. Sound Vib.* **2021**, *506*, 116178. [CrossRef]
23. Galvín, P.; Mendoza, D.L.; Connolly, D.P.; Degrande, G.; Lombaert, G.; Romero, A. Scoping Assessment of Free-Field Vibrations Due to Railway Traffic. *Soil Dyn. Earthq. Eng.* **2018**, *114*, 598–614. [CrossRef]
24. López-Mendoza, D.; Romero, A.; Connolly, D.P.; Galvín, P. Scoping Assessment of Building Vibration Induced by Railway Traffic. *Soil Dyn. Earthq. Eng.* **2017**, *93*, 147–161. [CrossRef]

25. Connolly, D.P.; Alves Costa, P.; Kouroussis, G.; Galvin, P.; Woodward, P.K.; Laghrouche, O. Large Scale International Testing of Railway Ground Vibrations across Europe. *Soil Dyn. Earthq. Eng.* **2015**, *71*, 1–12. [CrossRef]
26. He, C.; Zhou, S.; Guo, P.; Di, H.; Zhang, X. Modelling of Ground Vibration from Tunnels in a Poroelastic Half-Space Using a 2.5-D FE-BE Formulation. *Tunn. Undergr. Space Technol.* **2018**, *82*, 211–221. [CrossRef]
27. Zhou, S.; He, C.; Di, H.; Guo, P.; Zhang, X. An Efficient Method for Predicting Train-Induced Vibrations from a Tunnel in a Poroelastic Half-Space. *Eng. Anal. Bound. Elem.* **2017**, *85*, 43–56. [CrossRef]
28. Ma, M.; Liu, W.; Qian, C.; Deng, G.; Li, Y. Study of the Train-Induced Vibration Impact on a Historic Bell Tower above Two Spatially Overlapping Metro Lines. *Soil Dyn. Earthq. Eng.* **2016**, *81*, 58–74. [CrossRef]
29. Galvín, P.; Domínguez, J. Experimental and Numerical Analyses of Vibrations Induced by High-Speed Trains on the Córdoba–Málaga Line. *Soil Dyn. Earthq. Eng.* **2009**, *29*, 641–657. [CrossRef]
30. Liang, X.; Yang, Y.B.; Ge, P.; Hung, H.-H.; Wu, Y. On Computation of Soil Vibrations Due to Moving Train Loads by 2.5D Approach. *Soil Dyn. Earthq. Eng.* **2017**, *101*, 204–208. [CrossRef]
31. Cheng, G.; Feng, Q.; Sheng, X.; Lu, P.; Zhang, S. Using the 2.5D FE and Transfer Matrix Methods to Study Ground Vibration Generated by Two Identical Trains Passing Each Other. *Soil Dyn. Earthq. Eng.* **2018**, *114*, 495–504. [CrossRef]
32. Verbraken, H.; Lombaert, G.; Degrande, G. Verification of an Empirical Prediction Method for Railway Induced Vibrations by Means of Numerical Simulations. *J. Sound Vib.* **2011**, *330*, 1692–1703. [CrossRef]
33. Yang, J.; Zhu, S.; Zhai, W.; Kouroussis, G.; Wang, Y.; Wang, K.; Lan, K.; Xu, F. Prediction and Mitigation of Train-Induced Vibrations of Large-Scale Building Constructed on Subway Tunnel. *Sci. Total Environ.* **2019**, *668*, 485–499. [CrossRef]
34. Lopes, P.; Ruiz, J.F.; Alves Costa, P.; Medina Rodríguez, L.; Cardoso, A.S. Vibrations inside Buildings Due to Subway Railway Traffic. Experimental Validation of a Comprehensive Prediction Model. *Sci. Total Environ.* **2016**, *568*, 1333–1343. [CrossRef]
35. Guo, T.; Cao, Z.; Zhang, Z.; Li, A. Numerical Simulation of Floor Vibrations of a Metro Depot under Moving Subway Trains. *J. Vib. Control* **2018**, *24*, 4353–4366. [CrossRef]
36. Sanayei, M.; Zhao, N.; Maurya, P.; Moore, J.A.; Zapfe, J.A.; Hines, E.M. Prediction and Mitigation of Building Floor Vibrations Using a Blocking Floor. *J. Struct. Eng.* **2012**, *138*, 1181–1192. [CrossRef]
37. Sanayei, M.; Kayiparambil, P.A.; Moore, J.A.; Brett, C.R. Measurement and Prediction of Train-Induced Vibrations in a Full-Scale Building. *Eng. Struct.* **2014**, *77*, 119–128. [CrossRef]
38. Zou, C.; Moore, J.A.; Sanayei, M.; Wang, Y. Impedance Model for Estimating Train-Induced Building Vibrations. *Eng. Struct.* **2018**, *172*, 739–750. [CrossRef]
39. Zou, C.; Moore, J.A.; Sanayei, M.; Wang, Y.; Tao, Z. Efficient Impedance Model for the Estimation of Train-Induced Vibrations in over-Track Buildings. *J. Vib. Control* **2021**, *27*, 924–942. [CrossRef]
40. Zou, C.; Moore, J.A.; Sanayei, M.; Tao, Z.; Wang, Y. Impedance Model of Train-Induced Vibration Transmission Across a Transfer Structure into an Overtrack Building in a Metro Depot. *J. Struct. Eng.* **2022**, *148*, 04022187. [CrossRef]
41. Auersch, L. Building Response Due to Ground Vibration - Simple Prediction Model Based on Experience with Detailed Models and Measurements. *Int. J. Acoust. Vib.* **2010**, *15*, 101. [CrossRef]
42. Tao, Z.-Y.; Zou, C.; Yang, G.-R.; Wang, Y.-M. A semi-analytical method for predicting train-induced vibrations considering train-track-soil and soil-pile-building dynamic interactions. *Soil Dyn. Earthq. Eng.* **2023**, *167*, 107822. [CrossRef]
43. Li, X.; Chen, Y.; Zou, C.; Wu, J.; Shen, Z.; Chen, Y. Building coupling loss measurement and prediction due to train-induced vertical vibrations. *Soil Dyn. Earthq. Eng.* **2023**, *167*, 107644. [CrossRef]